ACS APPLIED MATERIALS & INTERFACES

Research Article

www.acsami.org

Constructing Robust Liquid Marbles for Miniaturized Synthesis of Graphene/Ag Nanocomposite

Ying Chu, Zhikui Wang, and Qinmin Pan*

School of Chemical Engineering and Technology, Harbin Institute of Technology, Harbin 150001, Heilongjiang, P. R. China

Supporting Information

ABSTRACT: Miniaturized synthesis is attracting much attention due to many potential applications; a challenge remains in exploring versatile microreactors capable of producing pure products. In this study, we reported a kind of thermally robust liquid marbles and their application for miniaturized synthesis of graphene/Ag nanocomposite. The liquid marbles were constructed by using superhydrophobic Fe_3O_4/C microsheets as encapsulating agents. Results revealed that the morphology of the encapsulating agent as well as the humidity of atmosphere strongly affected the robustness of liquid marbles at elevated temperature. The resulting graphene/Ag nanocomposite showed one of the best catalytic characteristics for 4-nitroaniline reduction among the reported catalysts. The findings of this study not only offer an alternative insight into the stability of liquid marbles at elevated temperature but also provide a facile strategy for miniaturized synthesis.

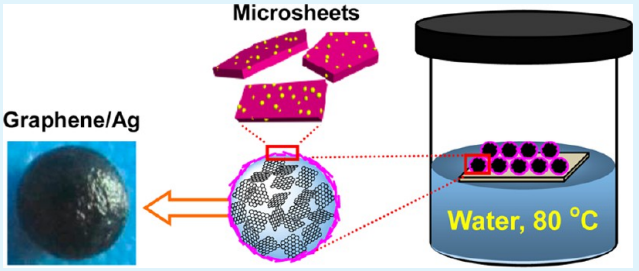

KEYWORDS: *miniaturized synthesis, liquid marble, superhydrophobic Fe_3O_4/C microsheets, graphene/Ag nanocomposite, catalytic reduction*

INTRODUCTION

Miniaturized synthesis has the advantages of reduced use of reactants, fast heat transfer rate, and controllable reaction conditions, which is very useful for biomedicine,[1,2] catalytic reaction,[3] sensor,[4,5] and material synthesis,[4,6] *etc.* Until now, a common strategy for miniaturized synthesis mainly involved the use of tiny liquid droplets as microreactors. These microreactors were constructed by several principles including water−oil emulsion,[7,8] microfluidic device,[9−11] and liquid droplets in immiscible fluid.[12−16] However, most of the reported approaches have shortcomings such as the instability of microreactors, the difficulty in controlling experimental conditions (temperature and humidity, *etc.*), and the contamination of final products, which limit their wide applications. Therefore, it is highly desirable to develop a facile method to construct microreactors capable of producing pure products.

Liquid marbles are liquid droplets (water, and glycerol, *etc.*) wrapped by hydrophobic[17−22] or hydrophilic[23−25] particles. Because of facile fabrication and suitability for various liquids, liquid marbles are considered as promising microreactors for chemical and biological processes. Miniaturized chemical reactions were recently conducted in liquid marbles at ambient temperature, including water pollution detection,[26] sensor,[27] chemiluminescence and photochemical polymerization,[28] and so on.[29,30] However, rare studies reported a miniaturized chemical process in liquid marbles at elevated temperature. A main reason for this lack is the collapse of liquid marbles caused by the evaporation of inner liquid at elevated temperature. To address this issue, nonvolatile liquids like ionic liquids[31] have been used as inner liquids in some marbles. On other hand, coating liquid droplets with multilayers of particles also reduced the evaporation of inner liquids.[18,28,32−44] Nevertheless, the multilayers formed by these particles exhibited porous structures, which could not effectively impede the escape of liquid molecules and thereafter the collapse of liquid marbles. Therefore, reducing the evaporation of inner liquid is crucial for improving the robustness of liquid marbles at elevated temperature.

Herein, we report a kind of robust liquid marbles that can be used for miniaturized synthesis of graphene-based nanocomposites. The liquid marbles were constructed by using superhydrophobic Fe_3O_4/C microsheets as encapsulating agent. By forming a compact layer on the surface of water droplets and elaborately controlling the humidity of atmosphere, the evaporation of inner water was greatly reduced at elevated temperature. As a result, graphene/Ag nanocomposite was synthesized in these liquid marbles, and it efficiently reduced 4-nitroaniline into *p*-phenylenediamine. The results of this study present an alternative insight into the thermal robustness of liquid marble, as well as a facile strategy for miniaturized synthesis.

EXPERIMENTAL SECTION

(1). Preparation of Superhydrophobic Fe_3O_4/C Microsheets. At first, monodispersed polystyrene (PS) microspheres with diameter of ~4.3 μm were synthesized according to a dispersion polymerization

Received: March 4, 2014
Accepted: April 11, 2014
Published: April 11, 2014

   dx.doi.org/10.1021/am501268g | ACS Appl. Mater. Interfaces 2014, 6, 8378−8386

Scheme 1. Illustration for the Fabrication of Fe_3O_4/C Microsheets

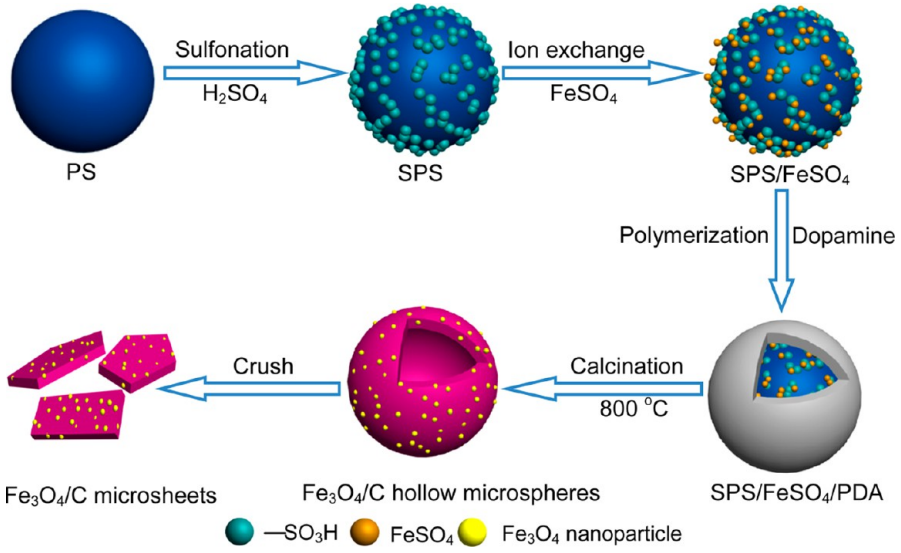

Scheme 2. Illustration for the Miniaturized Synthesis of Graphene/Ag Nanocomposite Using Liquid Marbles: (1) Construction of Liquid Marbles, (2) Reduction of GO/$AgNO_3$ Dispersion to Graphene/Ag Nanocomposite, (3) Separation, and (4) Collection of Graphene/Ag Nanocomposite from Superhydrophobic Fe_3O_4/C Microsheets

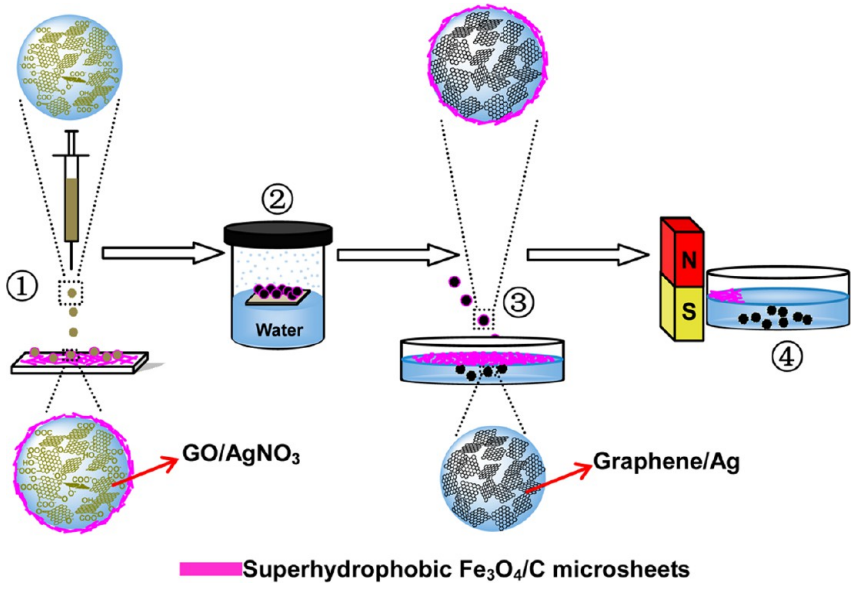

process.[45] The resulting PS microspheres (500 mg) were then treated with 50 mL of concentrated sulfuric acid (H_2SO_4, 98 wt %) at 40 °C for 4 h to obtain sulfonated PS (SPS) microspheres. After being washed with distilled water and ethanol, the obtained SPS microspheres were dispersed in 50 mL of distilled water at pH 11 and then 7.5 g of ferrous sulfate ($FeSO_4$) was added to the dispersion under stirring for 2 h. After being washed with distilled water, the resulting SPS/$FeSO_4$ microspheres were dispersed in 50 mL of tris(hydroxymethyl) aminomethane (Tris, 10 mM) solution containing 500 mg of dopamine hydrochloride (DA). The mixture was kept stirring at room temperature for 12 h. A layer of polydopamine (PDA) was coated on the surface of SPS/$FeSO_4$ microspheres. Then the resulting SPS/$FeSO_4$/PDA microspheres were calcinated at 800 °C with a heating rate of 2 °C min^{-1} for 2 h to prepare hollow Fe_3O_4/C microspheres (Figure S1, Supporting Information). The hollow Fe_3O_4/C microspheres were crushed with a mortar to fabricate Fe_3O_4/C microsheets. At last, the obtained Fe_3O_4/C microsheets were treated with 10 mM ethanol solution of *n*-dodecanethiol for 12 h (Scheme 1).

(2). Synthesis of Graphene/Ag Nanocomposite. Graphite oxide (GO) dispersion was prepared from natural graphite according to a modified Hummers' method.[46] Then 7-20 mg of silver nitrate ($AgNO_3$) and 14-21 mg of ascorbic acid (Vc)[47,48] were dissolved in 1 mL of GO dispersion (5 mg mL^{-1}) by ultrasonication for 15 min at room temperature. GO-based liquid marbles (~2 mm in diameter) were constructed by rolling droplets (~5 μL) of the resulting dispersion on a film of superhydrophobic Fe_3O_4/C microsheets. Then the liquid marbles were placed on a water bath at 80 °C for 50 min to reduce the dispersion into graphene/Ag nanocompoiste (Scheme 2, Figure S3 of supporting information). The resulting marbles were transferred to a water surface at room temperature to remove the superhydrophobic microsheets. After collecting the superhydrophobic microsheets by a magnet, black spherical graphene/Ag nanocomposite was left in the water. At last, the as-prepared nanocomposite was dialyzed in deionized water for 72 h to remove the residual Vc.

(3). Catalytic Reduction of 4-Nitroaniline. Spherical graphene/Ag nanocomposites (~100 mg) were added to 1.5 mL aqueous solution of 4-nitroaniline (0.1 mM) at room temperature. Then 2.5

dx.doi.org/10.1021/am501268g | ACS Appl. Mater. Interfaces 2014, 6, 8378−8386

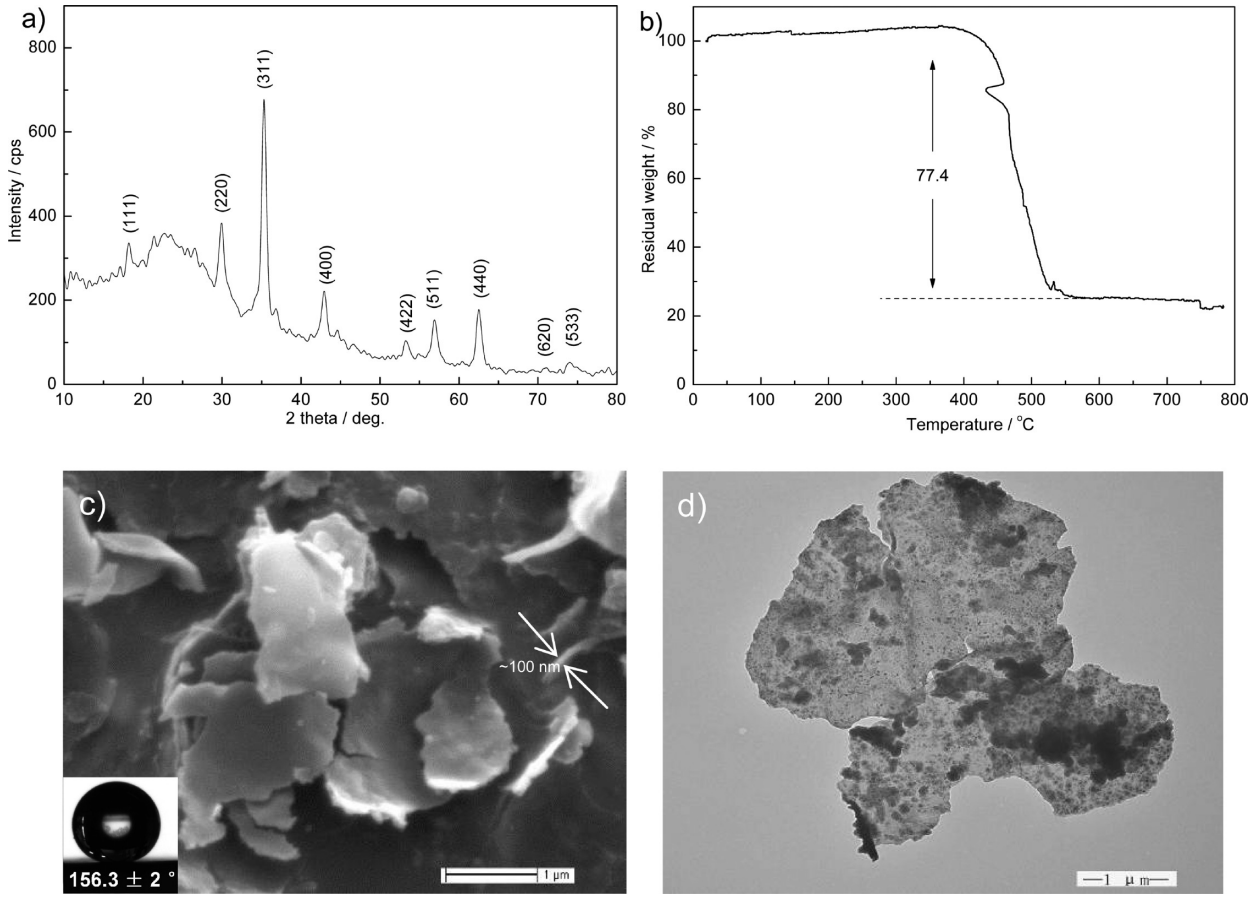

Figure 1. XRD pattern (a), TGA curve (b), SEM image (c), and TEM image (d) of superhydrophobic Fe_3O_4/C microsheets. Inset of part c is the water CA of the superhydrophobic microsheets.

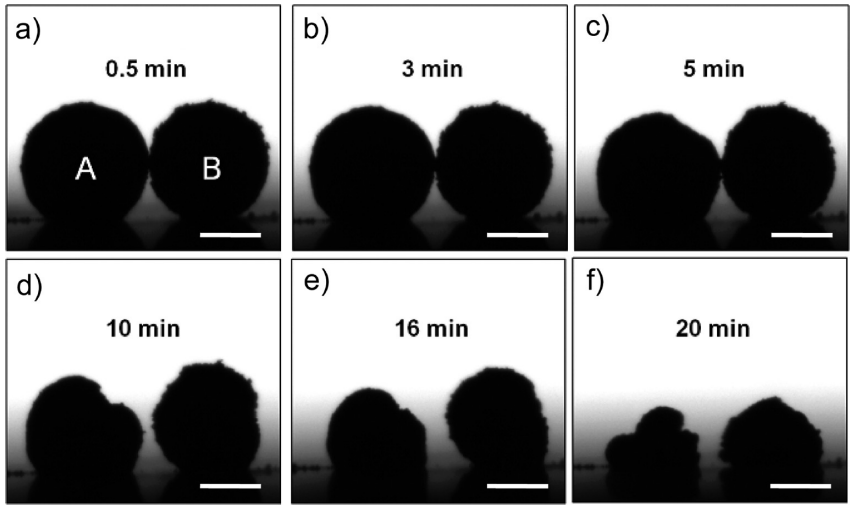

Figure 2. Horizontal profiles of the liquid marbles placed in atmosphere (20 °C, RH = ~50%) for (a) 0.5 min, (b) 3 min, (c) 5 min, (d) 10 min, (e) 16 min, and (f) 20 min. The marbles were constructed by superhydrophobic PS microspheres (left) and superhydrophobic Fe_3O_4/C microsheets (right). Scale bar: 1 mm.

mL of freshly prepared and ice-cooled sodium borohydride ($NaBH_4$, 0.02 mol L^{-1}) solution was added to the above mixture. Ultraviolet-visible absorption spectrometry was used to monitor the reduction of 4-nitroaniline.

(4). Characterizations. X-ray diffraction (XRD) patterns were obtained by a Shimadzu XRD-6000. Thermogravimetric analysis (TGA) was performed by using a Netzsch STA-449F3 in air at a heating rate of 10 °C min^{-1}. Scanning electron microscopy (SEM) images were recorded on a FEI Sirion 200. Transmission electron microscopy (TEM) observation was carried out on an H-7650 (Hitachi). Water contact angle (CA) was measured by an OCA20 (DataPhysics Instruments GmbH, Filderstadt). Two-dimensional (2D) and three-dimensional (3D) images of liquid marbles were obtained by a VHX-500 digital microscope (Keyence). The content of Ag in graphene/Ag nanocomposite was measured by 5300DV ICP (Perkin Elmer Optima). X-ray photoelectron spectroscopy (XPS) was

dx.doi.org/10.1021/am501268g | ACS Appl. Mater. Interfaces 2014, 6, 8378−8386

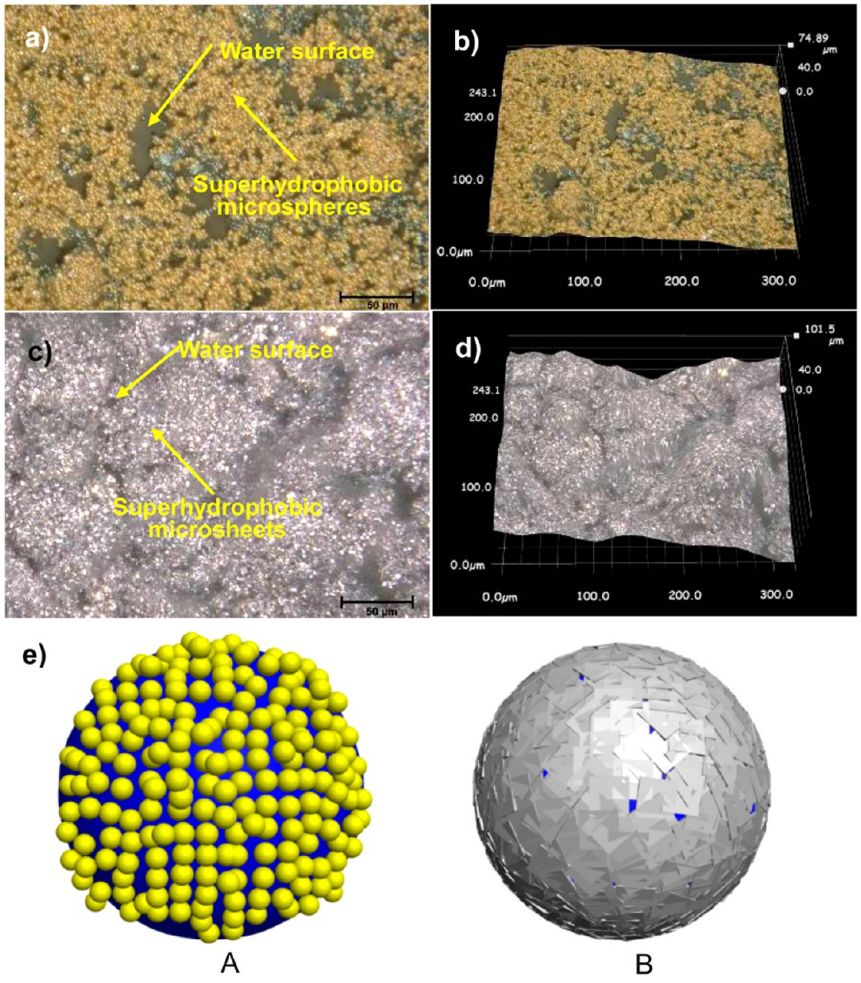

Figure 3. 2D (left) and 3D (right) images for the surface coatings on the liquid marbles constructed by superhydrophobic PS microspheres (a, b) and superhydrophobic Fe_3O_4/C microsheets (c, d). (e) Illustration for the encapsulation of a water droplet by superhydrophobic PS microspheres (A) and superhydrophobic Fe_3O_4/C microsheets (B).

performed on a PHI-5700 ESCA. Brunauer–Emmett–Teller (BET) surface area was measured by using a Micromeritics ASAP 2020. Ultraviolet-visible (UV-Vis) spectra were recorded by a SP-756P spectrophotometer (Shanghai Spectrum Instruments Co., Ltd, China).

RESULTS AND DISCUSSION

In order to construct robust liquid marbles, we used superhydrophobic Fe_3O_4/C microsheets as encapsulating agents in this study. Fe_3O_4/C microsheets were synthesized according to the procedure described in Scheme 1. At first, XRD, TGA, SEM, and TEM were employed to investigate the chemical composition and microstructure of the obtained Fe_3O_4/C microsheets. XRD pattern in Figure 1a displays the presence of Fe_3O_4 (JCPDS 65-3107) and amorphous carbon. The content of carbon phase in the microsheets was measured to be 77.4 wt % by TGA (Figure 1b). The SEM image in Figure 1c shows that these microsheets have a thickness of ~100 nm and lateral size of 1–2 μm. The TEM image in Figure 1d reveals the distribution of Fe_3O_4 nanoparticles on the microsheets. After modification with *n*-dodecanethiol, the microsheets exhibit superhydrophobicity and a water contact angle (CA) of 156.3 ± 2° (inset of Figure 1c).

Then the superhydrophobic microsheets were used to construct liquid marbles, and their robustness was investigated. Liquid marbles were constructed by rolling water droplets (~5 μL) on a film of superhydrophobic Fe_3O_4/C microsheets. The robustness of the marbles was measured by evaporation rate of inner water at ambient temperature. For comparison, similar experiments were also performed on liquid marbles constructed by using superhydrophobic polystyrene microspheres (PS, ~2.5 μm in diameter) as encapsulating agent (Figure S2, Supporting Information). We found that the morphology of encapsulating agent has an important impact on the robustness of the resulting marbles. At the same temperature and relative humidity (RH), a marble constructed by the microsheets exhibited better robustness than that fabricated by the microspheres, as shown in Figure 2. For example, the former still kept a spherical shape even when it was placed in atmosphere (20 °C, RH = ~50%) for 10 min, while the later started to collapse in 5 min under the same conditions, indicating a faster evaporation rate of inner water from the microsphere-constructed marble.

The difference in the evaporation rate is related to the compactness (or porosity) of encapsulating coatings on liquid droplets. This conclusion is supported by the appearance of encapsulating coatings recorded by a digital microscope. Figure 3a-d shows 2D and 3D digital images of the liquid marbles constructed by superhydrophobic PS microspheres and superhydrophobic Fe_3O_4/C microsheets, respectively. The images show that a lot of voids, a few to tens micrometers in size, are

dx.doi.org/10.1021/am501268g | ACS Appl. Mater. Interfaces 2014, 6, 8378–8386

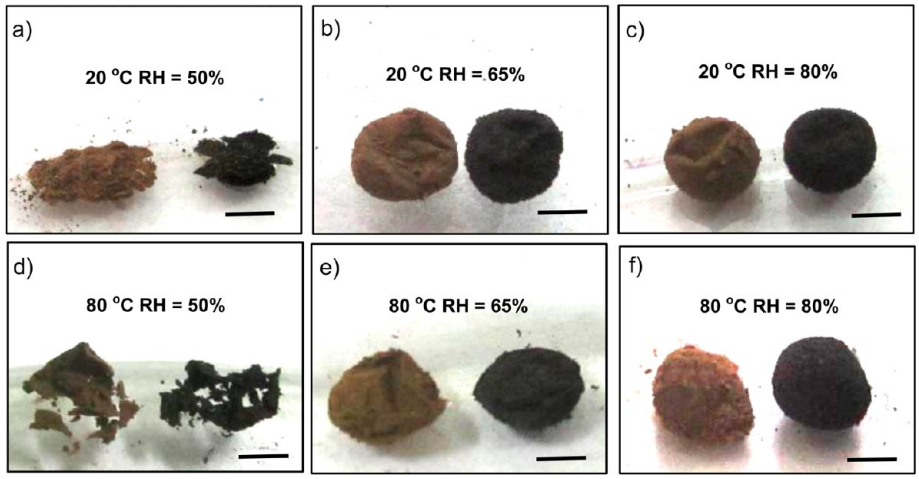

Figure 4. Optical images of the liquid marbles placed in atmosphere with different RH at 20 °C (a-c) and 80 °C (d-f) for 30 min. The marbles were constructed by superhydrophobic PS microspheres (left) and superhydrophobic Fe_3O_4/C microsheets (right). Scale bar: 1 mm.

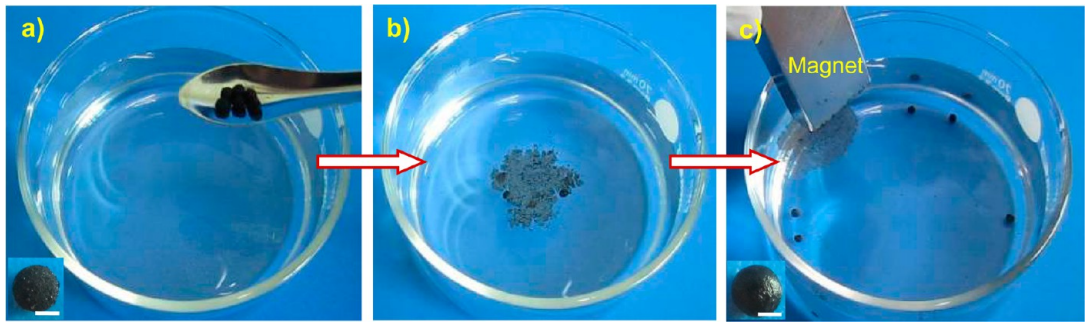

Figure 5. Optical images (a-c) for the separation of superhydrophobic Fe_3O_4/C microsheets from graphene/Ag nanocomposite on the water surface. Insets in parts a and c are the nanocomposite before and after the separation of the microsheets, respectively. Scale bar is 1 mm.

observed for the marbles constructed by the superhydrophobic microspheres (Figure 3a-b), indicating porous characteristic of the encapsulating coatings. The porous appearance not only reduces the compactness of the encapsulating coatings but also exposes inner water to air. As a result, the inner water evaporates through the voids and thus resulting in the collapse of the microsphere-constructed marbles. In contrast, there are only a few voids observed for the marbles constructed by the superhydrophobic microsheets (Figure 3c-d), indicating compact coatings on the surface of water droplets. It is reasonable that a compact coating lowers vapor permeability and reduces the evaporation rate of inner water to some extent, which is beneficial for the robustness of the marbles. Notably, the thickness of the encapsulating layers could not be measured due to curvature of the droplets. The above results suggest that the superhydrophobic microsheets are prone to stack into homogeneous and compact multilayers on the surface of water droplets compared with the microspheres, forming a more effective encapsulation for the droplets (Figure 3e).

We also found that relative humidity (RH) of atmosphere was an important factor affecting the robustness of the liquid marbles at elevated temperature. Figure 4 illustrates the shapes of the marbles placed in humid atmosphere at 20 and 80 °C for 30 min, respectively. In the atmosphere with RH of 50%, the marbles trend to shrink and even collapse at both 20 and 80 °C (Figure 4a and 4d), mainly caused by the fast evaporation of inner water. Nevertheless, the evaporation of inner water is significantly impeded by increasing the humidity of atmosphere to 65%. Indeed, only slight shrinkage is observed for the marbles placed in this atmosphere at 80 °C (Figure 4b and 4e). Interestingly, the marbles almost keep a spherical shape as the humidity rises to 80% even at 80 °C (Figure 4c and 4f).[49] Under the same conditions, marbles constructed by the superhydrophobic microspheres exhibit an irregular shape, also indicating that the morphology of encapsulating coatings plays an important role in evaporation rate of inner water. The reason is that high RH lowers the escaping tendency of water molecules, and a compact encapsulating layer also reduces the evaporation of inner water.[32,39] Recently, Matsukuma *et al.*[50] reported a film-like layer to diminish the porosity of encapsulating coatings, but this method was only carried out at room temperature. Therefore, the above results offer an alternative strategy for improving the robustness of liquid marbles at elevated temperature by using the superhydrophobic microsheets as encapsulating agent and keeping a humid atmosphere.

The as-prepared superhydrophobic microsheets were used for miniaturized synthesis of graphene/Ag nanocomposite (Scheme 2). In a typical experiment, liquid marbles were constructed by rolling the droplets of GO/$AgNO_3$/Vc dispersion on a film of superhydrophobic Fe_3O_4/C microsheets. Then the liquid marbles were placed in a water bath at 80 °C for 50 min to reduce the dispersion into graphene/Ag nanocomposite (Figure S3, supporting information). The RH of the bath surface was ~80%. As expected, these marbles were robust enough to withstand the heat treatment because neither

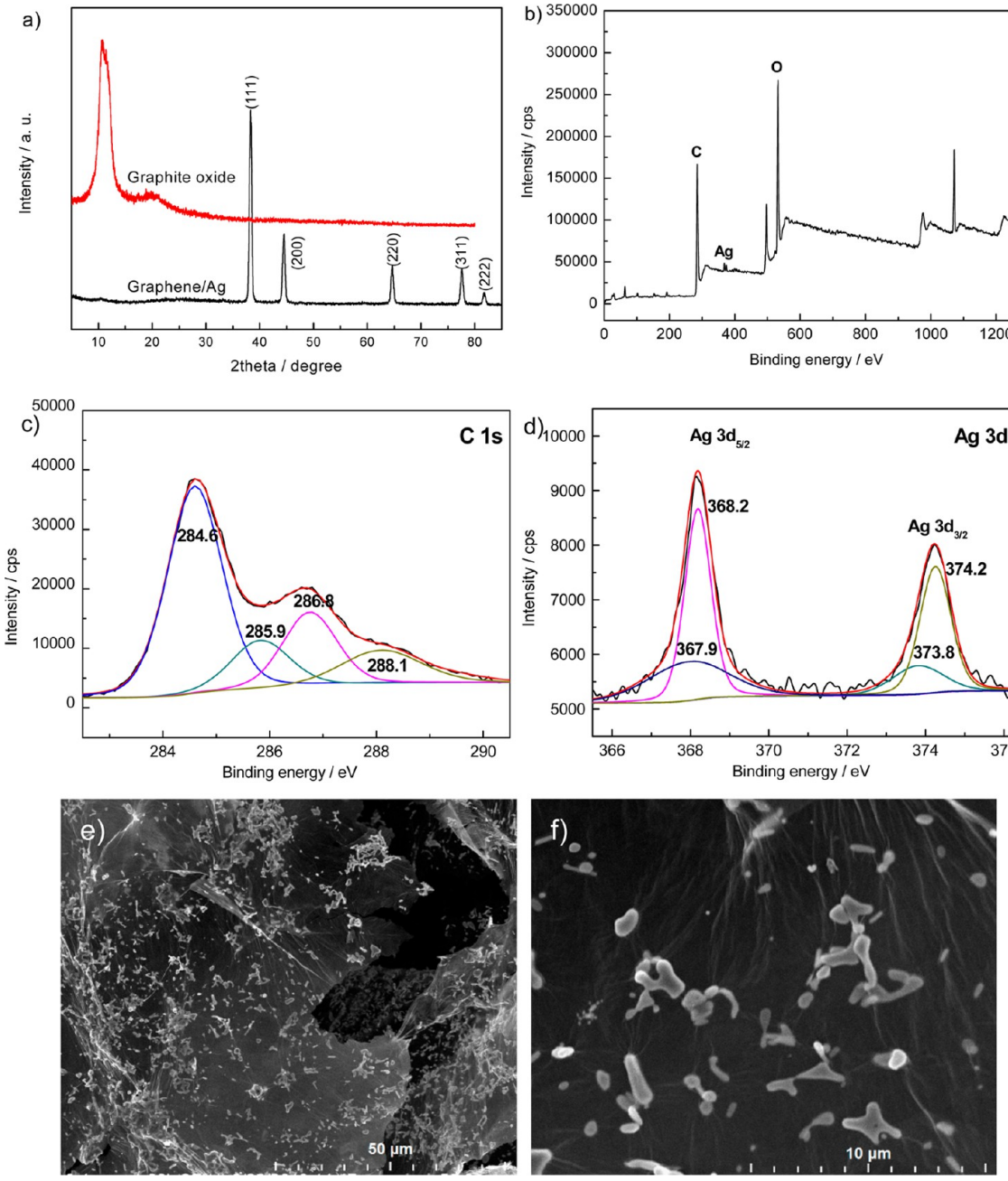

Figure 6. (a) XRD patterns of GO and the freeze-dried graphene/Ag nanocomposite. Survey scan (b), C 1s (c), Ag 3d (d) spectra, and SEM images (e, f) of the freeze-dried graphene/Ag nanocomposite; Ag/graphene mass ratio of the nanocomposite is 7.6.

shrinkage nor collapse occurred at the temperature range of 40−80 °C. After the reduction process, we obtained spheres coated with black superhydrophobic Fe_3O_4/C microsheets (inset of Figure 5a). Interestingly, the black microsheets could be easily detached by gently shaking the spheres on a water surface (Figure 5 and M1 of Supporting Information). After collecting the microsheets by a magnet, only spherical hydrogel with black and smooth appearance was left in the water (inset of Figure 5c).

The chemical and structural characteristics of the resulting nanocomposite after freeze-drying were investigated by XRD, XPS, and SEM measurements. XRD patterns in Figure 6a show feature peaks of Ag at 38.3° (111), 44.5° (200), 64.7° (220), 77.7° (311), and 81.8° (222), while no peaks of GO (10.6°) are observed for graphene/Ag nanocomposite, suggesting the reduction of GO, $AgNO_3$ into corresponding graphene and Ag. Figure 6b is the survey spectrum of the resulting graphene/Ag nanocomposite, which shows the elements of C, Ag, and O. The C 1s spectrum (Figure 6c) can be split into four components of C═C (284.6 eV), C−N (285.9 eV), C−O (286.8 eV), and C═O (288.1 eV).[51−53] Although the O-containing components are still observed for the nanocomposite, their peak intensities greatly decrease compared with those of GO.[47,48] We believe that the O-containing species mainly originate from the residual ascorbic acid and its oxidation product.[47,48] There are four peaks located at 368.2, 374.2, 367.9, and 373.8 eV in Ag 3d spectrum (Figure 6d), corresponding to the species of Ag(0) and Ag(I),[54] respectively. The morphology of graphene/Ag nanocomposite was investigated by SEM observations (Figure 6e-f). The SEM image in

dx.doi.org/10.1021/am501268g | ACS Appl. Mater. Interfaces 2014, 6, 8378−8386

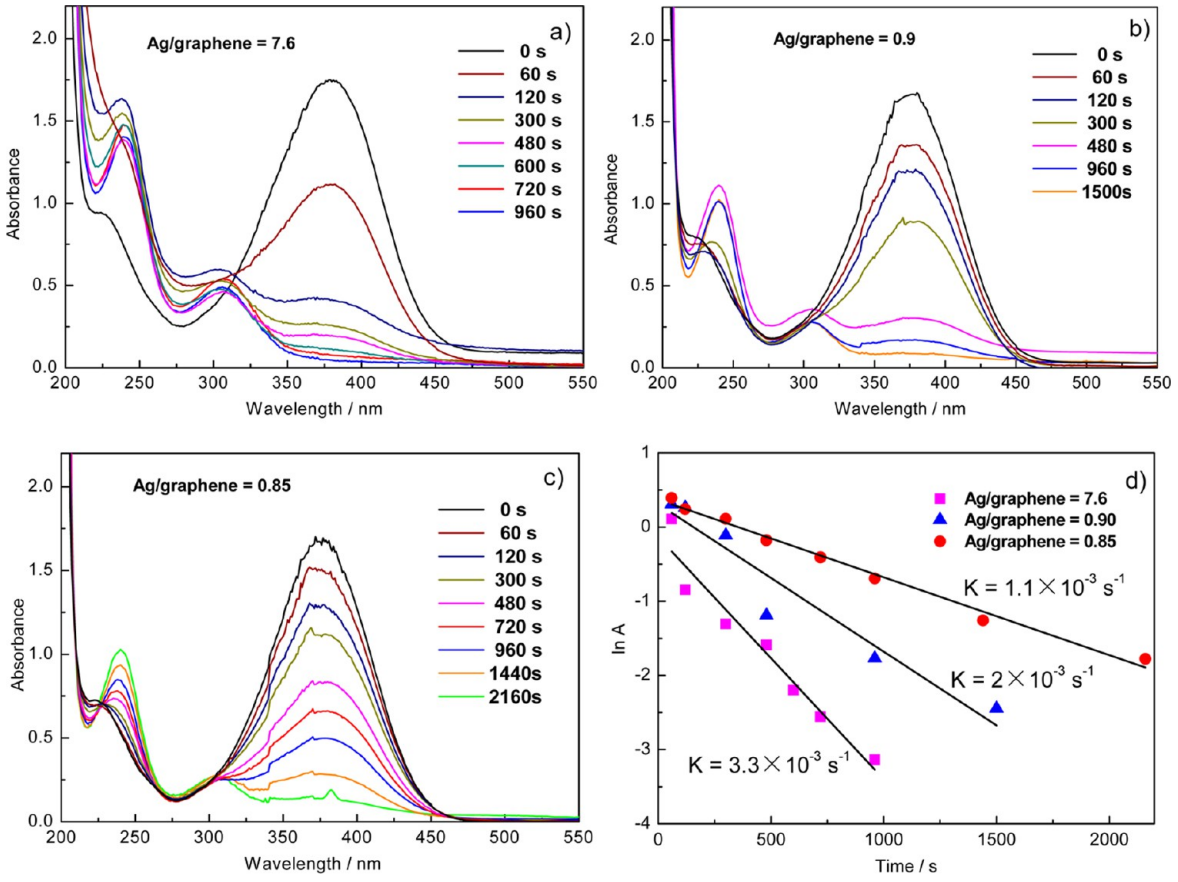

Figure 7. UV-Vis absorption spectra (a-c) and In A *vs* time plots (d) for the catalytic reduction of 4-nitroaniline by the nanocomposites with Ag/graphene mass ratio of (a) 7.6, (b) 0.90, and (c) 0.85.

Figure 6e shows that almost no residual Fe_3O_4/C microsheets cover on the outer surface of the nanocomposite, indicating complete separation of the microsheets. The complete separation suggests the weak interaction between the superhydrophobic microsheets and graphene/Ag nanocomposite, and thus avoiding the cross-contamination of the final product. High magnification SEM image displays that rod-like Ag nanoparticles uniformly cover on the surface of graphene sheets (Figure 6f). These graphene sheets interconnect into a porous architecture with BET surface area of 40.3 m^2 g^{-1}. The above results demonstrate the possibility for fabricating graphene-based nanomaterials through a miniaturized process by using liquid marbles as microreactors. Compared with conventional fabrication methods, the use of liquid marbles has advantages such as reduced use of chemicals, precisely controlled reaction conditions, high purity of product, and easy operation.

Application of the resulting graphene/Ag nanocomposite was demonstrated by the catalytic reduction of 4-nitroaniline to *p*-phenylenediamine. *p*-Phenylenediamine is an important chemical for the synthesis of textile and rubber antioxidants.[56] In this study, three kinds of nanocomposites with Ag/graphene mass ratio of 7.6, 0.90, and 0.85 were used to catalytic reduction of 4-nitroaniline, respectively. Figure 7a-c shows the dependence of UV-Vis absorption spectra on catalytic reduction time. Before the reaction, a strong absorption peak ascribed to 4-nitroaniline is located at ~380 nm. Then the peak diminishes quickly after introducing graphene/Ag nanocomposites to the aqueous solution of 4-nitroaniline/$NaBH_4$, indicating the occurrence of 4-nitroaniline reduction.[55] Meanwhile, absorption peaks of *p*-phenylenediamine appear at 240 and 305 nm. The reduction finishes in 960 s for the nanocomposite with an Ag/graphene mass ratio of 7.6. Figure 7d displays that In A and reaction time (t) exhibits a linear correlation, suggesting the pseudo-first-order kinetic model of the reduction process. The rate constant K of the nanocomposites for the reduction are 3.3 × 10^{-3} s^{-1} (Ag/graphene = 7.55), 2.0 × 10^{-3} s^{-1} (Ag/graphene = 0.90), and 1.1 × 10^{-3} s^{-1} (Ag/graphene = 0.85), respectively, which were calculated by the slopes of the fitted lines (Figure 7d). It is believed that porous architecture, high surface area, and uniformly dispersed Ag nanoparticles of the nanocomposites make the catalytic reduction fast and efficient. We also compared the present results with those of the previous studies. Traditional catalytic reduction of 4-nitroaniline was mostly conducted by using $PbBi_2Nb_2O_9$ nanocrystalline,[56] silver nanoparticles,[57,58] and so on, which had the drawbacks of low catalytic activity and poor stability. Additionally, complicated synthesis process and expensive reagents also limited the application of these catalysts. In contrast, these graphene/Ag nanocomposites not only exhibited one of the best catalytic performances for 4-nitroaniline reduction among the reported catalysts[56−58] but also were synthesized through a facile miniaturized chemical process.

CONCLUSIONS

In summary, this study reported the construction of thermally robust liquid marbles and their roles as reactors for the miniaturized synthesis of graphene/Ag nanocomposite. It was revealed that the morphology of encapsulating agent and the

dx.doi.org/10.1021/am501268g | ACS Appl. Mater. Interfaces 2014, 6, 8378−8386

humidity of atmosphere were important factors affecting the thermal stability of the liquid marbles, which provides an alternative insight into the robustness of liquid marbles at elevated temperature. Moreover, the obtained graphene/Ag nanocomposite showed one of the best catalytic characteristics for the reduction of 4-nitroaniline among the reported catalysts. With a choice of inner liquids, the strategy reported here might be extendable for miniaturized synthesis of functional materials that have potential applications in environment protection, catalysts, energy storage, and sensors, *etc.*

■ ASSOCIATED CONTENT

Supporting Information

SEM image of superhydrophobic Fe_3O_4/C hollow microspheres; the synthesis process, SEM image and water CA of superhydrophobic PS microspheres; the water bath for the preparation of graphene/Ag nanocomposite. This material is available free of charge via the Internet at http://pubs.acs.org.

■ AUTHOR INFORMATION

Corresponding Author

*E-mail: panqm@hit.edu.cn.

Notes

The authors declare no competing financial interest.

■ ACKNOWLEDGMENTS

This work was supported by Natural Science Foundation of China (05080313).

■ REFERENCES

(1) Abdelgawad, M.; Wheeler, A. R. The Digital Revolution: A New Paradigm for Microfluidics. *Adv. Mater.* **2009**, *21*, 920−925.
(2) Xiong, M.; Gu, B.; Zhang, J.; Xu, J.; Chen, H.; Zhong, H. Glucose Microfluidic Biosensors Based on Reversible Enzyme Immobilization on Photopatterned Stimuli-Responsive Polymer. *Biosens. Bioelectron.* **2013**, *50*, 229−234.
(3) Millsa, P. L.; Quiramb, D. J.; Ryley, J. F. Microreactor Technology and Process Miniaturization for Catalytic Reactions-A perspective on Recent Developments and Emerging Technologies. *Chem. Eng. Sci.* **2007**, *62*, 6992−7010.
(4) Jensen, K. F. Microreaction Engineering-Is Small Better? *Chem. Eng. Sci.* **2001**, *56*, 293−303.
(5) Manz, A.; Graber, N.; Widmer, H. M. Miniaturized Total Chemical Analysis Systems: a Novel Concept for Chemical Sensing. *Sens. Actuators, B* **1990**, *1*, 244−248.
(6) Srinivasan, R.; Hsing, I.; Berger, P. E.; Jensen, K. F. Micromachined Reactors for Catalytic Partial Oxidation Reactions. *AIChE J.* **1997**, *11*, 3059−3069.
(7) Obey, T. M.; Vincent, B. Novel Monodisperse "Silicone Oil"/Water Emulsion. *J. Colloid Interface Sci.* **1994**, *163*, 454−463.
(8) Fukui, Y.; Fujimoto, K. Bio-inspired Nanoreactor Based on a Miniemulsion System to Create Organic-Inorganic Hybrid Nanoparticles and Nanofilms. *J. Mater. Chem.* **2012**, *22*, 3493−3499.
(9) Peterson, D. S.; Rohr, T.; Svec, F.; Fréchet, J. M. J. Enzymatic Microreactor-on-a-Chip: Protein Mapping Using Trypsin Immobilized on Porous Polymer Monoliths Molded in Channels of Microfluidic Devices. *Anal. Chem.* **2002**, *74*, 4081−4088.
(10) Kobayashi, J.; Mori, Y.; Okamoto, K.; Akiyama, R.; Ueno, M.; Kitamori, T.; Kobayashi, S. A Microfluidic Device for Conducting Gas-Liquid-Solid Hydrogenation Reactions. *Science* **2004**, *304*, 1305−1308.
(11) Fujii, T. PDMS-Based Microfluidic Devices for Biomedical Applications. *Microelectron. Eng.* **2002**, *61*−*62*, 907−914.
(12) Alireza, A.; Nick, J. C.; Shin-Hyun, K.; David, A. W. Surface Functionalized Hydrophobic Porous Particles Toward Water Treatment Application. *Adv. Mater.* **2013**, *25*, 3215−3221.
(13) Shia-Yen, T.; Robert, L.; Lung-Hsin, H.; Abraham, P. L. Droplet Microfluidics. *Lab Chip* **2008**, *8*, 198−220.
(14) Chen, Y.; Nurumbetov, G.; Chen, R.; Ballard, N.; Bon, S. A. F. Multicompartmental Janus Microbeads from Branched Polymers by Single-Emulsion Droplet Microfluidics. *Langmuir* **2013**, *29*, 12657−12662.
(15) Mazutis, L.; Gilbert, J.; Ung, W. L.; Weitz, D. A.; Griffiths, A. D.; Heyman, J. A. Single-Cell Analysis and Sorting Using Droplet-Based Microfluidics. *Nat. Protoc.* **2013**, *8*, 870−891.
(16) Schneider, T.; Kreutz, J.; Chiu, D. T. The Potential Impact of Droplet Microfluidics in Biology. *Anal. Chem.* **2013**, *85*, 3476−3482.
(17) Aussillous, P.; Quéré, D. Liquid Marbles. *Nature* **2001**, *411*, 924−927.
(18) Aussillous, P.; Quéré, D. Properties of Liquid Marbles. *Proc. R. Soc. A* **2006**, *462*, 973−999.
(19) McHale, G.; Newton, M. I. Liquid Marbles: Principles and Applications. *Soft Matter* **2011**, *7*, 5473−5481.
(20) Bormashenko, E. Liquid Marbles: Properties and Applications. *Curr. Opin. Colloid Interface Sci.* **2011**, *16*, 266−271.
(21) Bormashenko, E. New Insights into Liquid Marbles. *Soft Matter* **2012**, *8*, 11018−11021.
(22) Bormashenko, E.; Pogreb, R.; Musin, A. Stable Water and Glycerol Marbles Immersed in Organic Liquids: From Liquid Marbles to Pickering-Like Emulsions. *J. Colloid Interface Sci.* **2012**, *366*, 196−199.
(23) Bormashenko, E.; Pogreb, R.; Musin, A.; Balter, R.; Whyman, G.; Aurbach, D. Interfacial and Conductive Properties of Liquid Marbles Coated with Carbon Black. *Powder Technol.* **2010**, *203*, 529−533.
(24) Bormashenko, E.; Pogreb, R.; Bormashenko, Y.; Musin, A.; Stein, T. New Investigations on Ferrofluidics: Ferrofluidic Marbles and Magnetic-Field-Driven Drops on Superhydrophobic Surfaces. *Langmuir* **2008**, *24*, 12119−12122.
(25) Dandan, M.; Erbil, H. Y. Evaporation Rate of Graphite Liquid Marbles: Comparison with Water Droplets. *Langmuir* **2009**, *25*, 8362−8367.
(26) Bormashenko, E.; Musin, A. Revealing of Water Surface Pollution with Liquid Marbles. *Appl. Surf. Sci.* **2009**, *255*, 6429−6431.
(27) Tian, J. F.; Arbatan, T.; Li, X.; Shen, W. Liquid Marble for Gas Sensing. *Chem. Commun.* **2010**, *46*, 4734−4736.
(28) Xue, Y.; Wang, H.; Zhao, Y.; Dai, L.; Feng, L.; Wang, X.; Lin, T. Magnetic Liquid Marbles: A "Precise" Miniature Reactor. *Adv. Mater.* **2010**, *22*, 4814−4818.
(29) Nakai, K.; Nakagawa, H.; Kuroda, K.; Fujii, S.; Nakamura, Y.; Yusa, S. Near-Infrared-Responsive Liquid Marbles Stabilised with Carbon Nanotubes. *Chem. Lett.* **2013**, *22*, 719−721.
(30) Bormashenko, E.; Balter, R.; Aurbach, D. Use of Liquid Marbles as Micro-Reactors. *Int. J. Chem. React. Eng.* **2011**, *9*, S10.
(31) Gao, L.; McCarthy, T. J. Ionic Liquid Marbles. *Langmuir* **2007**, *23*, 10445−10447.
(32) Laborie, B.; Lachaussée, F.; Lorenceau, E.; Rouyer, F. How Coatings with Hydrophobic Particles May Change the Drying of Water Droplets: Incompressible Surface versus Porous Media Effects. *Soft Matter* **2013**, *9*, 4822−4830.
(33) Pike, N.; Richard, D.; Foster, W.; Mahadevan, L. How Aphids Lose Their Marbles. *Proc. R. Soc. London, Ser. B* **2002**, *269*, 1211−1215.
(34) Eshtiaghi, N.; Liu, J. S.; Shen, W.; Hapgood, K. P. Liquid Marble Formation: Spreading Coefficients or Kinetic Energy? *Powder Technol.* **2009**, *196*, 126−132.
(35) Bhosale, P. S.; Panchagnula, M. V.; Stretz, H. A. Mechanically Robust Nanoparticle Stabilized Transparent Liquid Marbles. *Appl. Phys. Lett.* **2008**, *93*, 034109.
(36) Fujii, S.; Kameyama, S.; Armes, S. P.; Dupin, D.; Suzakia, M.; Nakamura, Y. pH-Responsive Liquid Marbles Stabilized with Poly(2-vinylpyridine) Particles. *Soft Matter* **2010**, *6*, 635−640.
(37) Bormashenko, E.; Pogreb, R.; Bormashenko, Y.; Musin, A.; Stein, T. New Investigations on Ferrofluidics: Ferrofluidic Marbles and

Magnetic-Field-Driven Drops on Superhydrophobic Surfaces. *Langmuir* **2008**, *24*, 12119−12122.
(38) Bormashenko, E.; Bormashenko, Y.; Musin, A.; Barkay, Z. On the Mechanism of Floating and Sliding of Liquid Marbles. *ChemPhysChem* **2009**, *10*, 654−656.
(39) Dandan, M.; Erbil, H. Y. Evaporation Rate of Graphite Liquid Marbles: Comparison with Water Droplets. *Langmuir* **2009**, *25*, 8362−8367.
(40) Wu, H.; Watanabe, H.; Ma, W.; Fujimoto, A.; Higuchi, T.; Uesugi, K.; Takeuchi, A.; Suzuki, Y.; Jinnai, H.; Takahara, A. Robust Liquid Marbles Stabilized with Surface-Modified Halloysite Nanotubes. *Langmuir* **2013**, *29*, 14971−14975.
(41) Larmour, I. A.; Saunders, G. C.; Bell, S. E. J. Sheets of Large Superhydrophobic Metal Particles Self Assembled on Water by the Cheerios Effect. *Angew. Chem., Int. Ed.* **2008**, *47*, 5043−5045.
(42) Hu, Y.; Jiang, H.; Liu, J.; Li, Y.; Hou, X.; Li, C. Highly Compressible Magnetic Liquid Marbles Assembled from Hydrophobic Magnetic Chain-Like Nanoparticles. *RSC Adv.* **2014**, *4*, 3162−3164.
(43) Dupin, D.; Armes, S. P.; Fujii, S. Stimulus-Responsive Liquid Marbles. *J. Am. Chem. Soc.* **2009**, *131*, 5386−5387.
(44) Zhang, L.; Cha, D.; Wang, P. Remotely Controllable Liquid Marbles. *Adv. Mater.* **2012**, *24*, 4756−4760.
(45) Tseng, C. M.; Lu, Y. Y.; Elaasser, M. S.; Vanderhoff, J. W. Uniform Polymer Particles by Dispersion Polymerization in Alcohol. *J. Polym. Sci., Polym. Chem.* **1986**, *24*, 2995−3007.
(46) Hummers, W. S.; Offeman, R. E. Preparation of Graphitic Oxide. *J. Am. Chem. Soc.* **1958**, *80*, 1339.
(47) Chen, W.; Yan, L. *In Situ* Self-Assembly of Mild Chemical Reduction Graphene for Three-Dimensional Architectures. *Nanoscale* **2011**, *3*, 3132−3137.
(48) Sui, Z.; Zhang, X.; Lei, Y.; Luo, Y. Easy and Green Synthesis of Reduced Graphite Oxide-Based Hydrogels. *Carbon* **2011**, *49*, 4314−4321.
(49) Erbil, H. Y. Evaporation of Pure Liquid Sessile and Spherical Suspended Drops: A Review. *Adv. Colloid Interface Sci.* **2012**, *170*, 67−86.
(50) Matsukuma, D.; Watanabe, H.; Minn, M.; Fujimoto, A.; Shinohara, T.; Jinnai, H.; Takahara, A. Preparation of Poly(lactic-acid)-Particle Stabilized Liquid Marble and the Improvement of Its Stability by Uniform Shell Formation Through Solvent Vapor Exposure. *RSC Adv.* **2013**, *3*, 7862−7866.
(51) Park, S.; Lee, K. S.; Bozoklu, G.; Cai, W.; Nguyen, S. T.; Ruoff, R. S. Graphene Oxide Papers Modified by Divalent Ions-Enhancing Mechanical Properties via Chemical Cross-Linking. *ACS Nano* **2008**, *2*, 572−578.
(52) Fan, Z. J.; Kai, W.; Yan, J.; Wei, T.; Zhi, L. J.; Feng, J.; Ren, Y. M.; Song, L. P.; Wei, F. Facile Synthesis of Graphene Nanosheets via Fe Reduction of Exfoliated Graphite Oxide. *ACS Nano* **2011**, *5*, 191−198.
(53) Chen, W.; Yan, L. Centimeter-Sized Dried Foam Films of Graphene: Preparation, Mechanical and Electronic Properties. *Adv. Mater.* **2012**, *24*, 6229−6233.
(54) Serghini-Monim, S.; Norton, P. R.; Puddephatt, R. J.; Pollard, K. D.; Rasmussen, J. R. Adsorption of a Silver Chemical Vapor Deposition Precursor on Polyurethane and Reduction of the Adsorbate to Silver Using Formaldehyde. *J. Phys. Chem. B* **1998**, *102*, 1450−1458.
(55) Chiu, C.; Chung, P.; Lao, K.; Liao, C.; Huang, M. H. Facet-Dependent Catalytic Activity of Gold Nanocubes, Octahedra, and Rhombic Dodecahedra toward 4-Nitroaniline Reduction. *J. Phys. Chem. C* **2012**, *116*, 23757−23763.
(56) Wu, W.; Liu, G.; Liang, S.; Chen, Y.; Shen, L.; Zheng, H.; Yuan, R.; Hou, Y.; Wu, L. Efficient Visible-Light-Induced Photocatalytic Reduction of 4-Nitroaniline Top-Phenylenediamine over Nanocrystalline $PbBi_2Nb_2O_9$. *J. Catal.* **2012**, *290*, 13−17.
(57) Pradhan, N.; Pal, A.; Pal, T. Silver Nanoparticle Catalyzed Reduction of Aromatic Nitro Compounds. *Colloids Surf., A* **2002**, *196*, 247−257.
(58) Zhou, Q.; Qian, G.; Li, Y.; Zhao, G.; Chao, Y.; Zheng, J. Two-Dimensional Assembly of Silver Nanoparticles for Catalytic Reduction of 4-Nitroaniline. *Thin Solid Films* **2008**, *516*, 953−956.